JOURNAL OF CATALYSIS 116, 338–349 (1989)

Kinetics and Mechanism of Catalytic Oxydehydrogenation of Alkylbenzenes

F. M. BAUTISTA, J. M. CAMPELO, A. GARCIA, D. LUNA, AND J. M. MARINAS

Department of Organic Chemistry, University of Cordoba, E-14004 Cordoba, Spain

Received June 21, 1988; revised October 25, 1988

The oxidative dehydrogenation of alkylbenzenes (ethylbenzene, *n*-propylbenzene, and isopropylbenzene) has been carried out at 673–823 K on the same nickel catalysts at 20 wt% supported on Al_2O_3, SiO_2, and two different types of $AlPO_4$ previously studied in nonoxidative conditions (F. M. Bautista *et al., J. Catal.* **107,** 181, 1987). Comparatively, the catalytic activity is not only higher in oxidative conditions but the alkylbenzene dehydrogenation is also able to take place on the supports conversely to what occurs in the absence of oxygen. This catalytic activity, unlike that obtained in nonoxidative conditions, is closely associated with the acid–base properties of the catalysts studied. In addition, a linear free-energy relationship was also obtained, manifesting itself through a "compensation effect" between $\Delta H^{\neq}$ and $\Delta S^{\neq}$ activation parameters obtained from the Eyring equation, similar to that previously described in nonoxidative conditions. On the basis of these results, we suggest for the oxydehydrogenation of alkylbenzenes a concerted mechanism through a common transition state which is produced by the transfer of two hydrogen atoms to a triplet oxygen molecule. The Lewis acid sites role consists of the catalytic activation of the oxygen molecule to the triplet state.

INTRODUCTION

The dehydrogenation of ethylbenzene to styrene is a very important industrial reaction carried out in vapor phase at 800–900 K on iron oxide stabilized with several promotors and in the presence of superheated steam which is used to provide the heat needed due to its endothermic character. The steam also reduces the partial pressures of substrates and keeps the catalyst clean and active (*1–4*). In addition, considerable work has been done in recent years (*4–8*) to produce catalytic systems where oxygen may function directly as a hydrogen acceptor yielding water as a by-product and providing the thermodynamic driving force for the reaction. Thus the reaction can be conducted at a lower temperature than without oxygen.

At the present time, most catalysts studied in this process are metallic oxides or several oxysalts ($ZrPO_4$, etc.) where the surface acid–base properties are closely related to their catalytic behavior (*7–11*). However, supported metal catalysts (*12–14*) are also able to produce ethylbenzene dehydrogenation through the reversal of the steps of a classical Horiuti–Polanyi type mechanism (*15*) describing the hydrogenation of an olefinic double bond. With respect to this, we studied (*16*) the nonoxidative dehydrogenation of several alkylbenzenes at 673–823 K on nickel catalysts at 20 wt% supported on Al_2O_3, SiO_2, and two different types of $AlPO_4$ synthesized according to Kearby (*17*). Our conclusion was that acid and basic sites did not exhibit catalytic activity in the nonoxidative conditions studied. However, the acid–base nature of the supports, through the effects of metal–support interaction, was found to play an important part in determining the catalytic activity of the supported nickel catalysts. These metal–support interaction effects in $AlPO_4$-supported nickel catalysts were previously obtained in the liquid-phase hydrogenation of the olefinic double bond (*18–24*) showing not only the importance of the role of the support in determin-

0021-9517/89 $3.00

ing the catalytic behavior of supported nickel systems but also the excellent behavior of $AlPO_4$ as nickel supports. Aluminum phosphates have also been used as supports for rhodium (*25, 26*), platinum (*27*), and palladium (*28*), respectively.

The present paper reports the results obtained in the oxidative dehydrogenation of the alkylbenzenes (R = Et, n-Pr, and i-Pr) over the same supported nickel systems previously employed as catalysts in the dehydrogenation of the same compounds (*16*) but in nonoxidative conditions, which will let us determine the influences of the reaction conditions (oxidative vs nonoxidative) on the performance of the catalysts studied.

On the other hand, $AlPO_4$ is structurally similar to silica (*29*) and exhibits a number of surface acid and basic sites (which may be controlled through synthetic procedure) and which have proved to act as catalysts in several reactions (*30–34*). Since the effect of the acid–base properties of oxides and oxysalts in the oxidative dehydrogenation of ethylbenzene has also been shown (*5–11, 35*), further research on this reaction may be of interest to compare the results obtained with the supported nickel catalysts and those obtained using each support as the catalyst.

EXPERIMENTAL

Catalyst

Systems containing 20 wt% nickel were prepared by impregnation of the supports to incipient wetness with 10 M aqueous solution of $Ni(NO_3)_2 \times 6H_2O$ following the procedure previously described (*16, 18, 20, 36*). They were dried, crushed, screened to a particle size <0.149 mm (100-mesh size), reduced in an ultrapure hydrogen stream (1.7 $cm^3\ s^{-1}$) at 673 K for 3 h, and then cooled to room temperature in the same hydrogen stream.

Four different supports have been used: commercial silica (SiO_2, Merck Kieselgel 60, 70–230 mesh), a commercial alumina (Al_2O_3, Merck acidic for chromatography), and two aluminium orthophosphates prepared according to Kearby (*17*) by precipitation from $Cl_3Al \times 6H_2O$ and H_3PO_4 (85 wt%) with aqueous ammonia ($AlPO_4$-F) or propylene oxide ($AlPO_4$-P), respectively. The pH value at the precipitation "endpoint" was in all cases 6.1 and the ratio Al/P = 1. The resulting powders screened to <0.149 mm were calcined in air at 920 K for 3 h. Both commercial supports, Al_2O_3 and SiO_2, were subjected to the same calcination treatment. A more detailed synthesis procedure and textural properties of supports, surface area, pore volume, and main pore diameter determined by nitrogen adsorption have been published elsewhere (*32, 33, 37*) and are summarized in Table 1, where the surface acidity and basicity of supports are also shown. These values were determined by a spectrophotometric method, previously described (*32, 33*), that allows titration of the amount of irreversibly adsorbed benzoic acid (pK_a = 4.19) or pyridine (pK_a = 5.25) employed as titrant agents of basic and acid sites, respectively.

Textural and acid–base properties of supported nickel catalysts have also been obtained in a similar way to that used with the supports and are summarized in Table 2, where the metal surface areas, S, of different catalysts are also shown. They were previously determined (*16, 36*) from the average crystallite diameter, D, obtained by X-ray diffraction, according to the method of Moss (*38*).

Apparatus, Materials, and Procedure

Oxidative dehydrogenation reactions were carried out in the same conventional fixed-bed type reactor previously described (*16*) with a continuous-flow system at atmospheric pressure. The reactor was made of stainless-steel tubing (15 mm in internal diameter and 120 mm long) placed in a tubular electric furnace and the prescribed temperature (673–823 K) was monitored by a thermocouple located in the reactor wall within an accuracy of ± 1 K. To obtain isothermal conditions, a known amount of

TABLE 1

Textural and Acid–Base Properties of the Different Supports

Support	S_{BET}[a] ($m^2\ g^{-1}$)	S_t[b] ($m^2\ g^{-1}$)	V[c] ($ml\ g^{-1}$)	d[d] (nm)	Acidity[e] ($\mu mol\ g^{-1}$)	Basicity[f] ($\mu mol\ g^{-1}$)
$AlPO_4$-P	228	236	0.94	2–4	227	166
$AlPO_4$-F	156	152	0.68	2–4	190	200
SiO_2	366	372	0.68	2–5	206	164
Al_2O_3	72	75	0.24	2–7	23	191

[a] Surface area, determined from BET method.
[b] Surface area from V-n plots.
[c] Pore volume.
[d] Main pore diameter.
[e] Monolayer coverage X_m at equilibrium at 298 K obtained with pyridine ($pK_a = 5.25$).
[f] Monolayer coverage X_m at equilibrium at 298 K obtained with benzoic acid ($pK_a = 4.19$).

fresh catalyst ($W = 0.1$ g < 0.149 mm) was diluted with glass beads and placed between two layers of glass beads separated by glass wool until the reactor was packed from top to bottom.

The standard pretreatment of the catalysts consisted of heating in a stream of 120 $cm^3\ min^{-1}$ nitrogen for 1 h at the reaction temperature. A stream of substrate vapor and oxygen was fed after dilution with nitrogen. In order to obtain different residence times $\tau = W/F$, defined as the ratio of the weight of the catalyst, W (g), to the feed rate, F ($mol\ s^{-1}$), at a fixed catalyst weight of 0.1 g, each substrate was fed at several rates (F in the interval 10–0.1 $cm^3\ min^{-1}$) by means of a microfeeder (Perfusor VI B. Braun) and at three different oxygen feed rates: 60, 80, and 100 $cm^3\ min^{-1}$, respectively.

In every case the amount of nitrogen was that which obtained a total feed rate ($O_2 + N_2$) of 120 $cm^3\ min^{-1}$.

The substrates ethyl- (EB), n-propyl- (n-PB), and isopropylbenzene (i-PB) from Merck p.a. were purified by distillation under reduced pressure and low temperature and then passed through active acidic aluminium oxide powder for chromatography (Merck) activated at 673 K in flowing ultrapure nitrogen. The reaction liquid products were collected by traps cooled with dry ice in acetone and analyzed on a 5720A Hewlett–Packard conventional gas chromatograph with a 2 m × 0.3 mm (i.d.) stainless-steel column packed with 5% poly-

TABLE 2

Acid–Base Properties, Surface Area, S_{BET}, Metal Surface Area, S, and Average Crystallite Diameter, D, of Supported 20 wt% Nickel Catalysts

Catalysts	D (nm)	S ($m^2\ g_{Ni}^{-1}$)	S_{BET} ($m^2\ g_{cat}^{-1}$)	Acidity[a] ($\mu mol\ g^{-1}$)	Basicity[b] ($\mu mol\ g^{-1}$)
Ni/$AlPO_4$-P	20.9	32.2	65	42	142
Ni/$AlPO_4$-F	11.9	55.6	78	40	159
Ni/SiO_2	15.1	44.5	264	106	82
Ni/Al_2O_3	25.2	26.8	60	15	178

[a] Pyridine, $pK_a = 5.25$.
[b] Benzoic acid, $pK_a = 4.19$.

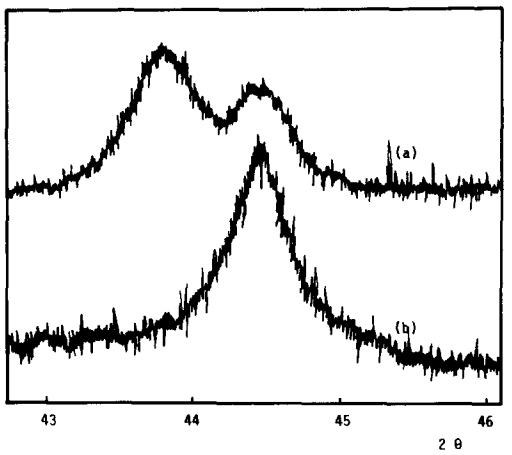

FIG. 1. X-ray diffraction profiles for Ni/$AlPO_4$-P catalyst after (a) and before (b) to be used in the dehydrogenation reactions described.

phenylether on Chromosorb G-AW DMCS 80/100. In addition, a spectrophotometric analysis of the different samples was made to the low conversion values obtained (<1%) at the higher F values. These experiments are developed at the wavelength of the maximum adsorption of the dehydrogenation products in cyclohexane solutions (spectroscopic grade, Merck). Both chromatographic and spectrophotometric analyses were the same as previously used in nonoxidative conditions (*16*), where as in the present case the only reaction products obtained were those corresponding to the dehydrogenation reaction of the alkylbenzenes: styrene, α-, and β-methylstyrene, respectively. However, in some experiments a very small amount of benzene was detected at the highest temperature.

With respect to the catalysts, partial oxidation of supported nickel metal is obtained in the present experimental conditions according to the X-ray diffraction patterns shown in Fig. 1. Here we can see the nickel metal peak as well as the nickel oxide peak (a) which is not present in the catalysts before the reaction (b). In addition, the presence of some nickel oxide in the catalyst used in nonoxidative conditions was not previously obtained (*16*).

RESULTS

The range of working conditions where no diffusional limitations exist (either internal or external) was that previously obtained (*16*) for the same catalysts in nonoxidative conditions. Thus, in the present experimental conditions the average particle size of the catalysts used (<0.149 mm) is the determining factor for the reaction not to be influenced by internal diffusion. Besides, substrate feed rates, F, over 1.2×10^{-4} mol s^{-1} determine the absence of external diffusion effects because the dehydrogenation rate is independent (within experimental error) with respect to F substrate values in the interval studied, $1.2\text{–}14 \times 10^{-4}$ mol s^{-1}. The reaction rates are also independent with respect to the oxygen feed rate studied for *n*-propyl and isopropylbenzene, respectively (Figs. 2b and 2c). However, as shown in Fig. 2a EB conversion is related to the oxygen feed rates. Thus, *n*-PB and *i*-PB data in Figs. 2b and 2c fit the identical rate equation previously obtained for the same catalysts under nonoxidative conditions,

$$X = k\tau, \tag{1}$$

while EB data fit the equation

$$X = k\tau P_{O_2}^n, \tag{2}$$

where X is the initial conversion degree, defined as the number of moles of dehydrogenated alkylbenzene per mole of alkylbenzene fed and n the reaction order with respect to partial oxygen pressure, P_{O_2} (in atm). The corresponding values of the reaction rate constants, k (in mol g^{-1} s^{-1}) obtained from both Eqs. (1) and (2), are collected in Table 3 for the three alkylbenzenes with the Ni/$AlPO_4$-P catalyst at 723 K. The reaction order with respect to P_{O_2}, $n = 0.7 \pm 0.1$, is also obtained from Eq. (2) for EB data.

The specific reaction rate constant values, k_S (in mol s^{-1} m^{-2}) defined as the activity per unit surface area of catalyst, are also shown. They are obtained from k and the

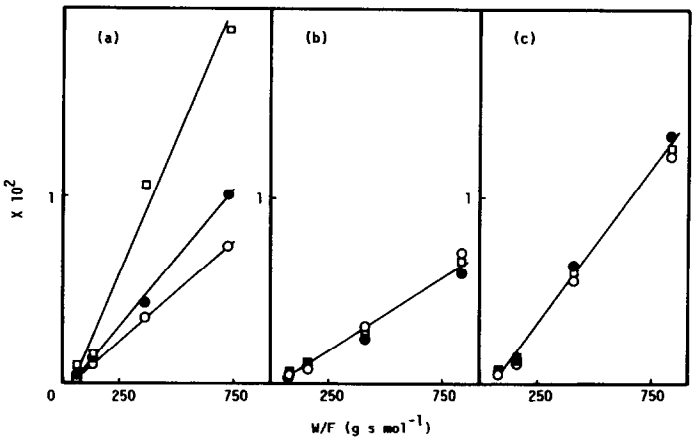

FIG. 2. Initial conversion degree, X, as a function of residence time, $\tau = W/F$, for (a) ethylbenzene, (b) *n*-propylbenzene, and (c) isopropylbenzene at three different oxygen feed rates: (○) 60, (●) 80, and (□) 100 $cm^3\ min^{-1}$, with the $Ni/AlPO_4$-P catalyst.

respective values of the BET surface area, S_{BET}, in Tables 1 and 2.

The results obtained in the temperature range studied are summarized in Fig. 3 where we can see the evolution of catalytic activity with temperature which lets us apply the Arrhenius equation obtaining the corresponding values of apparent activation energies, E_a, and Arrhenius constants, ln A, collected in Table 4.

In this connection, the Eyring equation also evaluates the temperature dependence of reaction rate constants in terms of transition state theory by separating the enthalpy, $\Delta H^{\neq}$, and entropy, $\Delta S^{\neq}$, components. Their corresponding values obtained by plotting ln (k/T) vs T^{-1} are also shown in Table 5.

DISCUSSION

The results collected in Table 3 and Fig. 3 show that the catalytic activities in the present experimental conditions are clearly higher (between 10 and 70 times, at 723 K, depending on the catalyst and the alkylbenzene) than those previously obtained (*16*) under identical experimental conditions using the same catalysts but in the absence of

TABLE 3

Reaction Rate Constants, k (mol $g^{-1}\ s^{-1}$), and Specific Reaction Rates, k_s (mol $s^{-1}\ m^{-2}$), of Different Catalysts in the Oxidative Dehydrogenation of Alkylbenzenes Studied under Standard Conditions at 723 K

Catalyst	Ethylbenzene		*n*-Propylbenzene		*i*-Propylbenzene	
	$10^7\ k$	$10^7\ k_s$	$10^7\ k$	$10^7\ k_s$	$10^7\ k$	$10^7\ k_s$
$AlPO_4$-P	125.4	0.55	20.5	0.09	58.4	0.26
$AlPO_4$-F	119.1	0.76	10.5	0.07	41.7	0.27
SiO_2	114.1	0.31	6.0	0.02	6.7	0.02
Al_2O_3	59.1	0.82	6.9	0.10	13.2	0.18
$Ni/AlPO_4$-P	531.2	8.17	78.7	1.21	169.3	2.61
$Ni/AlPO_4$-F	364.5	4.67	41.2	0.53	176.1	2.26
Ni/SiO_2	830.3	3.15	80.1	0.30	154.1	0.58
Ni/Al_2O_3	362.2	6.04	47.7	0.80	140.2	2.34

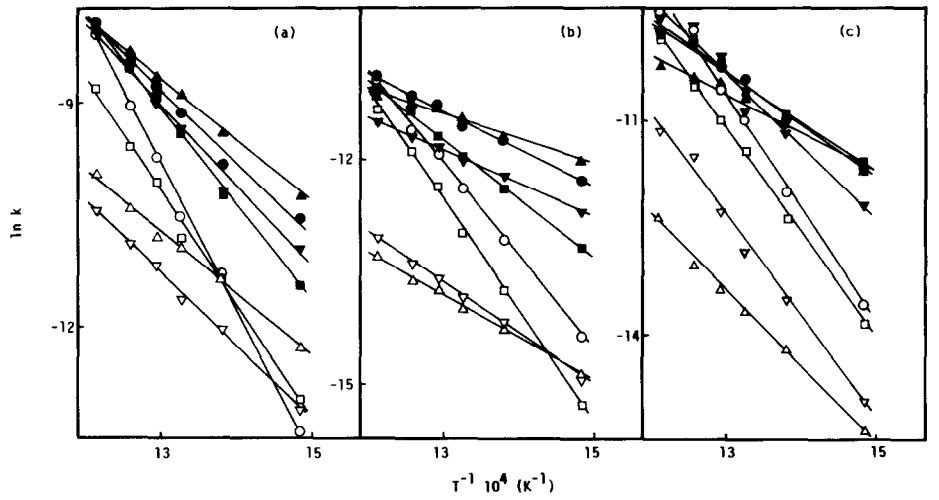

FIG. 3. Arrhenius plots for the oxidative dehydrogenation of (a) ethylbenzene, (b) *n*-propylbenzene, and (c) isopropylbenzene on different catalysts: (○) $AlPO_4$-P, (□) $AlPO_4$-F, (△) SiO_2, (▽) Al_2O_3, (●) Ni/$AlPO_4$-P, (■) Ni/$AlPO_4$-F, (▲) Ni/SiO_2, and (▼) NI/Al_2O_3.

oxygen (nonoxidative conditions). These differences increase sharply on increasing the reaction temperature. Here we also have to point out that $\Delta H^{\neq}$ and $\Delta S^{\neq}$ values increase to the same extent as the catalytic activity, EB > *i*-PB > *n*-PB, while in nonoxidative conditions the opposite occurs (*16*). Thus, the influence of electronic and steric effects of the methyl substitution (associated with $\Delta H^{\neq}$ and $\Delta S^{\neq}$ values, respectively) promotes different effects on the catalytic activity depending on the oxygen participation in the dehydrogenation reaction. In addition, in the actual oxidative conditions, alkylbenzene dehydrogenation is able to take place on the surface of different supports, unlike in nonoxidative conditions where the catalytic activity was exclusively developed on the nickel metal surface (*16*).

Consequently we have to consider that both the oxidative and the nonoxidative de-

TABLE 4

Apparent Activation Energies, E_a (kJ mol^{-1}), and Arrhenius Constants, ln *A* (mol s^{-1} g^{-1}), for the Catalysts and Substrates Studied

Catalyst	Ethylbenzene		*n*-Propylbenzene		*i*-Propylbenzene	
	E_a	ln *A*	E_a	ln *A*	E_a	ln *A*
$AlPO_4$-P	162 ± 5	15.5 ± 0.8	104 ± 1	4.3 ± 0.1	132 ± 6	10.0 ± 1.0
$AlPO_4$-F	126 ± 5	9.5 ± 0.8	122 ± 2	6.8 ± 0.4	121 ± 2	8.0 ± 0.4
SiO_2	69 ± 3	0.0 ± 0.5	47 ± 2	−6.4 ± 0.3	89 ± 3	0.6 ± 0.4
Al_2O_3	81 ± 2	1.4 ± 0.4	57 ± 2	−4.7 ± 0.2	120 ± 6	6.6 ± 0.9
Ni/$AlPO_4$-P	81 ± 4	3.9 ± 0.6	42 ± 2	−4.7 ± 0.4	60 ± 3	−0.8 ± 0.4
Ni/$AlPO_4$-F	106 ± 3	7.5 ± 0.6	65 ± 2	−1.5 ± 0.3	58 ± 2	−1.2 ± 0.4
Ni/SiO_2	68 ± 2	2.0 ± 0.3	28 ± 2	−7.0 ± 0.4	45 ± 3	−3.6 ± 0.4
Ni/Al_2O_3	93 ± 6	5.0 ± 1.0	37 ± 1	−6.0 ± 0.8	85 ± 7	3.0 ± 1.0

Note. Uncertainties are determined by standard deviations.

TABLE 5

Activation Enthalpies, $\Delta H^{\neq}$ (kJ mol^{-1}), and Activation Entropies, $\Delta S^{\neq}$ (J mol^{-1} K^{-1}), for the Catalysts and the Substrates Studied

Catalyst	Ethylbenzene		*n*-Propylbenzene		*i*-Propylbenzene	
	$\Delta H^{\neq}$	$\Delta S^{\neq}$	$\Delta H^{\neq}$	$\Delta S^{\neq}$	$\Delta H^{\neq}$	$\Delta S^{\neq}$
$AlPO_4$-P	156 ± 5	−133 ± 7	97 ± 1	−225 ± 1	126 ± 6	−176 ± 9
$AlPO_4$-F	120 ± 5	−183 ± 6	116 ± 2	−205 ± 3	115 ± 2	−194 ± 3
SiO_2	63 ± 3	−262 ± 4	41 ± 2	−313 ± 2	83 ± 3	−255 ± 4
Al_2O_3	75 ± 2	−250 ± 3	51 ± 2	−299 ± 2	113 ± 6	−207 ± 8
Ni/$AlPO_4$-P	75 ± 4	−229 ± 5	36 ± 2	−299 ± 3	54 ± 3	−267 ± 3
Ni/$AlPO_4$-F	100 ± 4	−200 ± 5	59 ± 2	−272 ± 2	52 ± 2	−270 ± 3
Ni/SiO_2	62 ± 2	−245 ± 3	22 ± 2	−318 ± 3	39 ± 3	−290 ± 4
Ni/Al_2O_3	87 ± 6	−216 ± 8	31 ± 1	−310 ± 1	79 ± 7	−235 ± 9

Note. Uncertainties are determined by standard deviations.

hydrogenation processes of alkylbenzenes are developed through two different kinds of mechanisms. However, the concerted character of the oxidative process actually studied can also be accounted for by consideration of the kinetic parameters presented in Tables 4 and 5 as previously obtained for the nonoxidative process (*16*). Thus, the negative values of $\Delta S^{\neq}$ indicate that, on going from the ground state to the transition state, an extensive restriction in the degrees of freedom must be considered. A highly ordered transition state and the relatively low $\Delta H^{\neq}$ values here obtained are consistent with a concerted evolution in the limiting adsorption step.

Thus, the difference between the oxidative process actually studied and the nonoxidative one can be ascribed not to its concerted character (because they both exhibit this character) but to the participation of the oxygen molecule in the transition state (TS) determining the limiting step. In this sense, we can see in Fig. 4 how the kinetics parameters $\Delta H^{\neq}$ vs $\Delta S^{\neq}$ for oxidative (values in Table 5) and nonoxidative conditions

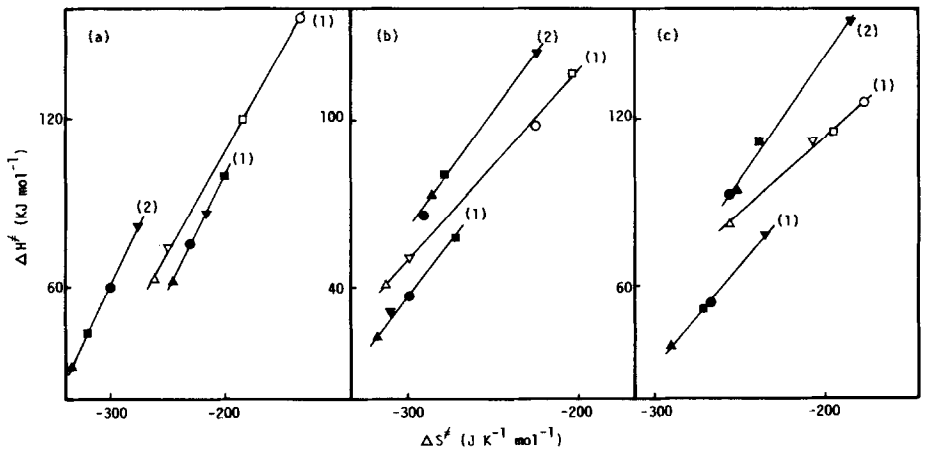

FIG. 4. Compensation effect between $\Delta H^{\neq}$ and $\Delta S^{\neq}$ for (a) ethylbenzene, (b) *n*-propylbenzene, and (c) isopropylbenzene in the oxidative conditions of this work (1) and in the nonoxidative conditions (2). The symbols of different catalysts are the same as for Fig. 3.

TABLE 6

Values of ln α_S and θ_S^a (K) Obtained from the Representation of ln A vs E_a and Values of θ_S^b (K), $\Delta G_S^{\neq}$ (kJ mol^{-1}), and ln $K_S^{\neq}$, Obtained from the Representation of $\Delta H^{\neq}$ vs $\Delta S^{\neq}$ with the Different Catalysts

	Ethylbenzene		*n*-Propylbenzene		*i*-Propylbenzene	
	Supports	Ni/supports	Supports	Ni/supports	Supports	Ni/supports
ln α_S	−12.0 ± 0.6	−8.0 ± 0.1	−14.8 ± 0.7	−11.3 ± 0.5	−19.0 ± 2.0	−10.8 ± 0.3
θ_S^a	709 ± 21	825 ± 8	672 ± 28	794 ± 57	552 ± 49	733 ± 22
θ_S^b	708 ± 21	825 ± 9	675 ± 28	793 ± 56	544 ± 45	738 ± 22
$\Delta G_S^{\neq}$	250 ± 4	265 ± 2	251 ± 7	275 ± 17	222 ± 9	252 ± 6
ln $K_S^{\neq}$	−42 ± 1	−38.6 ± 0.5	−45 ± 2	−42 ± 4	−49 ± 5	−41 ± 2

(*16*) fit three different straight lines: one corresponding to supports and the other two to supported nickel catalysts in oxidative and nonoxidative conditions, respectively. So, like that obtained in nonoxidative conditions (*16*) an enthalpy–entropy relationship exists in the present case that may be ascribed to the existence of a linear free-energy relationship (LFER)

$$\Delta G_{\text{const}}^{\neq} = -\theta R \ln K^{\neq} = \Delta H^{\neq} - \theta \Delta S^{\neq} \tag{3}$$

known as the "compensation effect" or the "isokinetic relationship" (IKR) (*39–41*) although the most habitual representation is through the equation

$$\ln A = \ln \alpha + E_a/\theta R, \tag{4}$$

where R is the gas constant, θ the isokinetic temperature at which identical values of reaction rate constant $k = \alpha$ are obtained, $K^{\neq}$ the equilibrium constant of the activated complex, and $\Delta G^{\neq}$ the activation free energy. Consequently, the values of isokinetic parameters for each substrate (θ_S, α_S, $K_S^{\neq}$, and $\Delta G_S^{\neq}$) (Table 6) are obtained from slopes and intercepts in Eqs. (3) and (4) by plotting ln A vs E_a in Table 4 and $\Delta H^{\neq}$ vs $\Delta S^{\neq}$ in Table 5 for each substrate with the two sets of catalysts for the oxidative process as shown in Fig. 4: supports and supported nickel catalysts, respectively.

Furthermore, if an IKR holds for a reaction series, a single common interaction mechanism can be expected (*39, 42, 43*) also exhibiting the same value of activation free energy, $\Delta G^{\neq}$, over the experimental temperature range. According to this and on the basis of the experimental results shown in Fig. 4, we conclude that two different kinds of concerted mechanism exist in the dehydrogenation of alkylbenzenes in oxidative and nonoxidative conditions. In addition, the fact that higher $\Delta S^{\neq}$ values are always obtained in the oxidative process than in the nonoxidative process for a given $\Delta H^{\neq}$ value in Fig. 4 points out that the formation of the activated complex in actual oxidative conditions is accompanied by an additional entropy which is consistent with oxygen molecule participation in the TS formation. This fact may also account for the comparatively increased values of catalytic activity in the oxidative process since for a common ($-\Delta H^{\neq}$/RT) value (identical catalyst and reaction temperature) the corresponding value of the other exponential component of the reaction rate ($\Delta S^{\neq}$/R) will always be higher in oxidative than in nonoxidative conditions.

The results shown in Fig. 4 also manifest the existence of a different mechanism in the oxidative dehydrogenation process when it is carried out on supports or on supported nickel systems. Such a difference may be ascribed in this case to the differential role played by the acid–base sites in both catalysts thus determining very different $\Delta G_{\text{const}}^{\neq}$ values for each set of

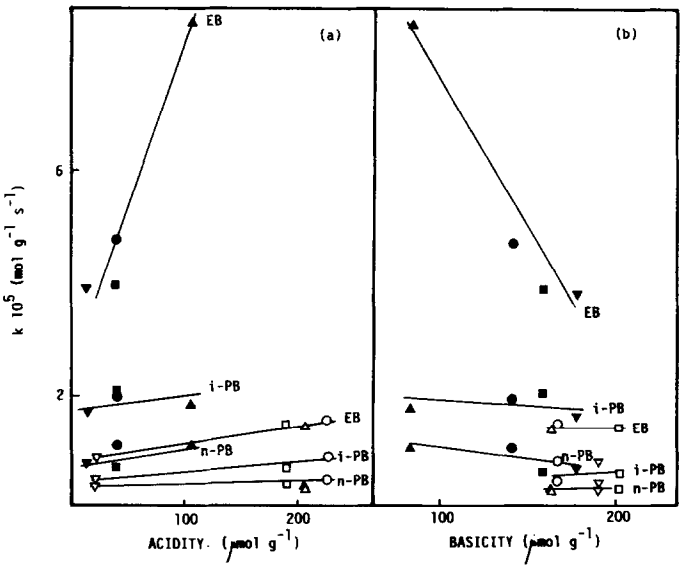

FIG. 5. Influence of the acidity (a) and basicity (b) properties of different catalysts (collected in Tables 1 and 2) on the dehydrogenation rate of different alkylbenzenes at 723 K (shown in Table 3). The symbols for different catalysts are the same as in Figs. 3 and 4.

reactions. In fact, on plotting k values in Table 3 against the acidity and basicity values in Tables 1 and 2, respectively, we obtain that (Fig. 5) both acid and basic sites are closely associated to catalytic activity (especially in the ethylbenzene dehydrogenation process) although this influence of acid and basic sites is clearly different for each set of catalysts. Thus, acid sites enhance catalytic activity in both cases but to a very different extent. Basic sites, according to results shown in Fig. 5b, diminish activity in the supported nickel systems while their effects on the supports as catalysts seem to be negligible. These results are consistent with those presented by Pines (*44*) referring to the existence of a fine balance between acidic and basic sites in nonsupported nickel catalysts with a variable proportion of nickel oxide.

Accordingly, in many previous works the role of acid sites was emphasized either for the oxydehydrogenation itself (*5, 6, 9*) or for the formation of active coke on the catalyst surface where the oxydehydrogenation process is properly developed (*7, 8, 10*). It is also reported that both surface sites (on inorganic solids and on coke) could participate in the dehydrogenation process using nickel phosphate as the catalyst (*11*). Even some peculiar distribution of acid–base pairs on this solid was considered advantageous for coke formation, and hence for subsequent acceleration of the reactions (*35*). However, whichever the case is the Lewis acid character of the active sites has been recently demonstrated (*11*).

In this respect, the role of Lewis acid as catalyst in some concerted processes, such as the Diels–Alder reaction or "ene" synthesis, has already been established (*45–47*) and it is also interesting to note that the active coke characterized as a polynaphthoquinone (*7, 8*) was produced by a double cycloaddition (a Diels–Alder and an intramolecular ene process, respectively) between two styrene molecules followed by an oxidative oxygen insertion, probably throughout an endoperoxide intermediate. In addition, the mechanism for the oxydehydrogenation of ethylbenzene by this coke with quinoid groups is assumed to be a

quinoid redox system where the reduction of quinoid groups is carried out by the transfer of two hydrogen atoms from ethylbenzene, thus obtaining a styrene molecule. The hydroquinoid systems are oxidized by an oxygen molecule and the quinoid group is regenerated. However, the interaction between ethylbenzene and quinoid groups, according to the model considered in this paper (*7*), may be assumed as an allowed concerted hydrogen transfer.

Taking into account that our kinetic study prompts us to consider a concerted evolution of the transition state in the limiting step and the presence of a dark black carbonaceous material deposited on the surface of the initially white supports when they are used as catalysts, we could suggest an identical mechanism to that proposed for the oxidative dehydrogenation of ethylbenzene on crystalline zirconium phosphate (*7, 8*) for oxidative dehydrogenation of the alkylbenzene studied.

However, at the present time we can tentatively consider the existence of another concerted mechanism carried out directly on the Lewis acid sites of the catalyst which according to Brozyna and Dziewcki (*11*) could produce alkylbenzene dehydrogenation at the same time that active coke does. This concerted mechanism considers the direct transfer of two hydrogen atoms to a triplet oxygen molecule. Activation to the triplet state is produced by the action of Lewis acid sites (Fig. 6).

This possibility arises from the results reported on a Lewis acid catalyzed addition of triplet oxygen to 1,3 dienes yielding the corresponding endoperoxide in a way similar to a Diels–Alder reaction (*48*). Thus, the oxygen adsorption on a Lewis acid site overcomes the spin barrier, which lets it participate in a concerted hydrogen transfer process through a six-membered cyclic transition state just as the cycloaddition to endoperoxides does (Step I). In this connection, the ability of $SiO_2 \cdot Al_2O_3$ catalysts to activate gaseous oxygen has been described by using ESR measurements (*6, 49*). Under the experimental conditions studied, the hydrogen transfer of alkylbenzenes to hydrogen peroxide (Step II), which gives rise to a new alkenylbenzene and two water molecules, is the fastest step and ought not to be necessarily a catalyzed reaction.

The presence of coke and other secondary products may be explained in the context of the present mechanism by the action of a nonspecific oxidant agent like hydrogen peroxide over the alkenylbenzenes.

CONCLUSIONS

On the basis of this study we can conclude that the gas-phase oxydehydrogenation of alkylbenzenes exhibits a LFER

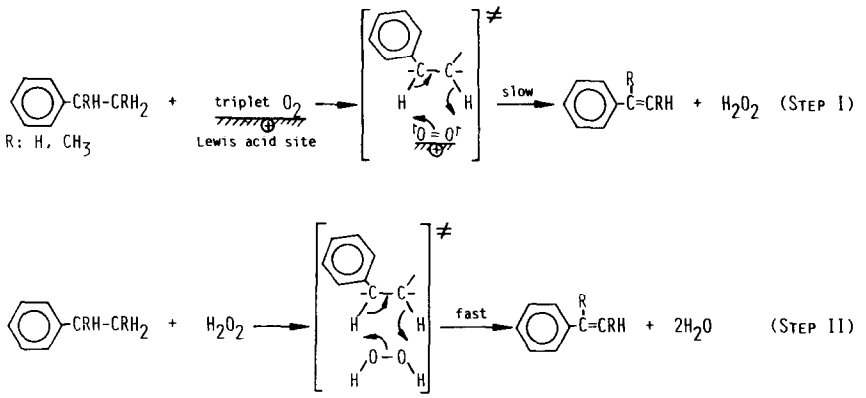

FIG. 6. Concerted reaction mechanism proposed for the oxydehydrogenation of the alkylbenzenes studied.

(manifesting itself through a linear relationship between the activation parameters $\Delta H^{\neq}$ and $\Delta S^{\neq}$ known as compensation effect) as that obtained in the same experimental, though nonoxidative, conditions. So a series of θ, $\Delta G^{\neq}$, $K^{\neq}$, and α isokinetic parameters have been obtained which provide a general measurement of catalytic behavior as well as valuable information on the reaction mechanism.

On the other hand, the gas-phase dehydrogenation mechanism in nonoxidative as well as in oxidative conditions can be explained within the framework of a concerted process. However, in the first case the mechanism was consistent (*16*) with the reversal of steps describing the hydrogenation of an olefinic double bond where, according to Ponec (*50*), the interaction with the supported nickel catalyst enables the removal of symmetry restrictions imposed by Woodward–Hoffman rules in these thermally forbidden pericyclic reactions. Conversely, the reaction mechanism in oxidative conditions can be described as a hydrogen transfer to quinoid groups of an active coke and/or to an activated triplet oxygen molecule by the action of the Lewis acid sites of the catalyst. These two different mechanisms are able to explain the differential behavior of supports in both reaction conditions. That is, while supports do not act as catalysts in nonoxidative conditions, in the presence of an oxygen stream they become excellent catalysts, especially both $AlPO_4$ studied.

ACKNOWLEDGMENTS

The financial aid of the Dirección General de Investigación Cientifica y Técnica del Ministerio de Educación y Ciencia de España, Proyecto PA86-0065, is gratefully acknowledged. Also the authors wish to acknowledge the grammatical revision of the manuscript carried out by M. Sullivan.

REFERENCES

1. Rylander, P. N., "Catalysis Science and Technology" (J. R. Anderson and M. Boudart, Eds.), Vol. 4, Chap. 1, p. 17. Springer-Verlag Chemie, Berlin, 1983.
2. Pines, H., "The Chemistry of Catalytic Hydrocarbon Conversions," Chap. 4, p. 208. Academic Press, New York, 1981.
3. Lee, E. H., *Catal. Rev.* **8,** 285 (1973).
4. Kung, H., *Ind. Eng. Chem. Prod. Res. Dev.* **25,** 171 (1986).
5. Murakami, Y., Iwayama, K., Uchida, H., Hattori, T., and Tagawa, T., *Appl. Catal.* **2,** 67 (1982).
6. Tagawa, T., Iwayama, K., Ishida, Y., Hattori, T., and Murakami, Y., *J. Catal.* **79,** 47 (1983).
7. Emig, G., and Hofmann, H., *J. Catal.* **84,** 15 (1983).
8. Schraut, A., Emig, G., and Sockel, H. G., *Appl. Catal.* **29,** 311 (1987).
9. Hattori, T., Hanai, H., and Murakami, Y., *J. Catal.* **84,** 294 (1979).
10. Fiedorow, R., Przystajko, W., Sopa, M., and Della Lana, I. G., *J. Catal.* **68,** 33 (1981).
11. Brozyna, K., and Dziewcki, *Appl. Catal.* **35,** 211 (1987).
12. Bailey, H. C., Williamson, J. B., and Capp, C. W., British Patent 1,098,697 (Sept. 17, 1965).
13. Fujimoto, K., and Kunugi, T., *Ind. Eng. Chem. Prod. Res. Dev.* **20,** 319 (1981).
14. Duprez, D., Miloudi, A., Delahay, G., and Maurel, R., *J. Catal.* **101,** 56 (1986).
15. Horiuti, I., and Polanyi, P., *Trans. Faraday Soc.* **30,** 1164 (1934).
16. Bautista, F. M., Campelo, J. M., Garcia, A., Luna, D., and Marinas, J. M., *J. Catal.* **107,** 181 (1987).
17. K. Kearby, *in* "Proceedings, 2nd International Congress on Catalysis, Paris, 1960," p. 2567. Technip, Paris, 1961.
18. Campelo, J. M., Garcia, A., Luna, D., and Marinas, J. M., *Appl. Catal.* **3,** 315 (1982).
19. Campelo, J. M., Garcia, A., Luna, D., and Marinas, J. M., *Bull. Soc. Chim. Belg.* **92,** 851 (1983).
20. Campelo, J. M., Garcia, A., Gutierrez, J. M., Luna, D., and Marinas, J. M., *Appl. Catal.* **7,** 307 (1983).
21. Marcelin, G., and Vogel, R. F., *J. Catal.* **82,** 482 (1983).
22. Marcelin, G., Vogel, R. F., and Swift, H. E., *J. Catal.* **83,** 42 (1983).
23. Campelo, J. M., Garcia, A., Luna, D., and Marinas, J. M., *J. Chem. Soc. Faraday Trans. I* **80,** 695 (1984).
24. Marcelin, G., Vogel, R. F., and Swift, H. E., *J. Catal.* **98,** 64 (1986).
25. Cabello, J. A., Campelo, J. M., Garcia, A., Luna, D., and Marinas, J. M., *J. Catal.* **94,** 1 (1985).
26. Cabello, J. A., Campelo, J. M., Garcia, A., Luna, D., and Marinas, J. M., *J. Org. Chem.* **51,** 1786 (1986).
27. Aramendia, M. A., Borau, V., Jimenez, C., Marinas, J. M., and Rodero, F., *Bull. Chem. Soc. Japan* **60,** 3415 (1987).

28. Alba, A., Aramendia, M. A., Borau, V., Jimenez, C., and Marinas, J. M., *J. Catal.* **98,** 288 (1986).
29. Mooney, R. C. L., *Acta Crystallogr.* **9,** 728 (1956).
30. Moffat, J. B., *Catal. Rev. Sci. Eng.* **18,** 199 (1978).
31. Itoh, H., Tada, A., and Hattori, H., *J. Catal.* **76,** 235 (1982).
32. Campelo, J. M., Garcia, A., Gutierrez, J. M., Luna, D., and Marinas, J. M., *Canad. J. Chem.* **61,** 2567 (1983).
33. Campelo, J. M., Garcia, A., Luna, D., and Marinas, J. M., *Canad. J. Chem.* **62,** 638 (1984).
34. Cabello, J. A., Campelo, J. M., Garcia, A., Luna, D., and Marinas, J. M., *J. Org. Chem.* **49,** 5195 (1984).
35. Dziewiecki, Z., and Makowski, A., *React. Kinet. Catal. Lett.* **31,** 9 (1986).
36. Campelo, J. M., Garcia, A., Luna, D., and Marinas, J. M., *J. Catal.* **97,** 108 (1986).
37. Campelo, J. M., Garcia, A., Gutierrez, J. M., Luna, D., and Marinas, J. M., *Colloids Surf.* **8,** 353 (1984).
38. Moss, R. L., "Experimental Methods in Catalytic Research" (R. B. Anderson and P. T. Dawson, Eds.) Vol. 2, Chap. 2, p. 43. Academic Press, New York, 1976.
39. Conner, W. C., Jr., *J. Catal.* **78,** 238 (1982).
40. Galwey, A. K., *J. Catal.* **84,** 270 (1983).
41. Bond, G. C., *Z. Phys. Chem. N. F.* **144,** 21 (1985).
42. Linert, W., Soukup, R. W., and Schmidt, R., *Comp. Chem.* **6,** 47 (1982).
43. Galwey, A., and Brown, M., *J. Catal.* **60,** 335 (1979).
44. Pines, H., *in* "Advances in Catalysis," Vol. 35, p. 323. Academic Press, New York, 1987.
45. Houk, K. N., and Strozier, R. W., *J. Amer. Chem. Soc.* **95,** 4094 (1973).
46. Snider, B. B., *J. Org. Chem.* **39,** 255 (1974).
47. Alston, P. V., and Ottembrite, R. M., *J. Org. Chem.* **40,** 1111 (1975).
48. Barton, D. H. R., Haynes, R. K., Leclerc, G., Magnus, P. D., and Menzies, I. D., *J. Chem. Soc. Perkin Trans. 1,* 2055 (1975).
49. Tagawa, T., Hattori, T., and Murakami, Y., *J. Catal.* **75,** 66 (1982).
50. Ponec, R., *Collect. Czech. Chem. Commun.* **51,** 1843 (1986).